Acta Biochim Biophys Sin 2022, 54(9): 1349–1364
https://doi.org/10.3724/abbs.2022126
Advance Access Publication Date: 8 September 2022
Original Article

Original Article

A novel small positive allosteric modulator of neuropeptide receptor PAC1-R exerts neuroprotective effects in MPTP mouse Parkinson's disease model

Guangchun Fan[1,†], Shang Chen[1,†], Zhengxin Tao[1], Huahua Zhang[5], and Rongjie Yu[1,2,3,4,*]

[1]Department of Cell Biology, College of Life Science and Technology, Jinan University, Guangzhou 510630, China, [2]Guangdong Province Key Laboratory of Bioengineering Medicine, Guangzhou 510630, China, [3]Guangdong Provincial Biotechnology Drug & Engineering Technology Research Center, Guangzhou 510630, China, [4]National Engineering Research Center of Genetic Medicine, Guangzhou 510630, China, and [5]Department of Medical Genetics, Guangdong Medical University, Dongguan 523000, China

[†]These authors contributed equally to this work.

*Correspondence address. Tel: +86-13392625921; E-mail: rongjie_yu1123@163.com/tyrj@jnu.edu.cn

Received 12 April 2022 Accepted 21 June 2022

Abstract

As a neuropeptide pituitary adenylate cyclase-activating polypeptide (PACAP)-preferring receptor, PAC1-R mediates effective neuroprotective activity. Based on the finding that the antibiotic doxycycline (DOX) with clinical neuroprotective activity functions as a positive allosteric modulator (PAM) of neuropeptide PACAP receptor 1 (PAC1-R), we use virtual and laboratory screening to search for novel small molecule PAMs of PAC1-R. Virtual screening is carried out using a small-molecule library TargetMol. After two-level precision screening with Glide, the top five compounds with the best predicted affinities for PAC1-R are selected and named small positive allosteric modulator 1–5 (SPAM1–5). Our results show that only 4-{[4-(4-Oxo-3,4-2-yl)butanamido]methyl}benzoic acid (SPAM1) has stronger neuroprotective activity than DOX in the MPP+ PD cell model and MPTP PD mouse model. SPAM1 has a higher affinity for PAC1-R than DOX, but has no antibiotic activity. Moreover, both SPAM1 and DOX block the decrease of PAC1-R level in mouse brain tissues induced by MPTP. The successful screening of SPAM1 offers a novel drug for the treatment of neurodegenerative disease targeting the PAC1-R.

Key words positive allosteric modulator, PACAP receptor 1, doxycycline, computer virtual screening, neuroprotective activity, Parkinson's disease

Introduction

PACAP (pituitary adenylate cyclase-activating polypeptide) was first isolated from ovine hypothalamic extract on the basis of its ability to stimulate cAMP formation in anterior pituitary cells. It belongs to the vasoactive intestinal polypeptide (VIP)/secretin/growth hormone releasing hormone/glucagon superfamily [1]. PACAP receptor 1 (PAC1-R) belongs to class B G-protein-coupled receptors (GPCRs). Unlike the other two types of receptors of PACAP, *i.e.*, VPAC1-R and VPAC2-R, which are shared by both PACAP and VIP, PAC1-R has almost 1000 folds higher affinity for PACAP than for VIP [2]. As a PACAP-preferring receptor, PAC1-R is abundantly expressed in the central nervous system and peripheral nervous system and mediates the significant anti-inflammatory [3], anti-apoptotic [4], neuroprotective [5] and neurogenetic [6] activities of PACAP. Therefore, PAC1-R has been considered as an important drug target in the treatment of neurodegenerative diseases, including Alzheimer's disease and Parkinson's disease (PD) [7,8].

The small molecular antibiotic doxycycline (DOX) and its derivative minocycline have been reported to have significant anti-inflammatory [9], anti-apoptosis [5,10] neuroprotective [11] and neurogenetic [12] activities, which are considered as potent neuroprotective agents against neurodegenerative diseases [13,14]. Our previous reports confirmed that both DOX and minocycline bind to the same allosteric modulation site in the N-terminal extracellular domain of PAC1-R (PAC1-EC1) and work as positive allosteric modulators (PAMs) of PAC1-R and exert neuroprotective effects by enhancing the activation of the neuropeptide receptor PAC1-R [15,16]. Our data indicated the existence of a positive allosteric modulation site in PAC1-EC1, and the effective binding at this positive allosteric modulation site by doxycycline and minocycline can

promote the activation of PAC1-R, which contributes to their neuroprotective activities. Based on these findings, we hypothesized that there may be some other small molecules that can also bind to the same positive allosteric modulation site in the PAC1-EC1 domain as DOX. The successful screening of novel small molecular PAMs (SPAMs) of PAC1-R which have stronger positive allosteric modulatory activity targeting PAC1-R and less antibiotic side effect than DOX may benefit the development of new drugs targeting PAC1-R for the treatment of neurodegenerative diseases such as PD.

In the present study, we firstly used computer virtual screening to search for novel small molecular chemical candidates from the TargetMol small molecule library, which can target the same positive allosteric modulation site in the PAC1-EC1 domain recognized by DOX. Then, the cell model of PD with 1-methyl-4-phenylpyridinium (MPP +) was used to screen the small molecules with more potent cytoprotective activity than DOX against the apoptosis induced by MPP + in SH-SY5Y cells from the candidates obtained from the virtual screening. After that, the theoretical and laboratory affinities targeting PAC1-EC1 and the antibiotic activities were compared between the candidate SPAMs and DOX. Furthermore, the 1-methyl-4-phenyl-1,2,3,6-tetrahydropyridine (MPTP) mouse model of PD was further used to verify the neuroprotective effect of the candidate SPAMs *in vivo*. Finally, immunohistochemistry assay of brain tissues, including the substantia nigra and corpus striatum, was performed to verify the relationship between the neuroprotective activities of SPAMs and PAC1-R levels.

Materials and Methods

Chemicals and cells

MPTP (M0896), methylthiazoletetrazolium bromide (MTT) (M5655), MPP + (M7068), DA (PHR1090), 3,4-dihydroxyphenylacetic acid (DOPAC) (11569), homovanillic acid (HVA) (H1252) and DOX were purchased from Sigma–Aldrich (St Louis, USA). Chemicals including Enamine_Z71395360 (SPAM1), Enamine_Z594413782 (SPAM2), Enamine_Z87576051 (SPAM3), Enamine_Z1762997274 (SPAM4), and Enamine_Z1916181887 (SPAM5) were obtained from Enamine Company (Kyiv, Ukraine). The peptides PACAP38, PACAP(6–38) and PACAP(28–38) were synthetized by GL Biochem (Shanghai, China), with a purity of 95 % confirmed by reversed-phase high-performance liquid chromatography (HPLC) and matrix-assisted laser desorption/ionization time of flight (MALDI-TOF) mass spectrometry. The human neuroblastoma cell line SH-SY5Y was obtained from the Shanghai Institutes for Biological Sciences (Shanghai, China).

Homology modelling of PAC1-R

In this work, only the extracellular N-terminus and seven-transmembrane domain of the human PAC1-R were modelled, because the intracellular C-terminus is unrelated to the binding of small molecules to PAC1-R. The resolved 3D protein crystal structure (PDB ID: 2JOD), which is the complex structure of PAC1-EC1 and PACAP(6–38), was used as the extracellular domain template, and the crystal structure of human glucagon class B G protein coupled receptor (PDB ID: 4L6R) was selected as the template to model the seven-transmembrane region of PAC1-R. Homology modelling was performed using the Modeler program in the Discovery Studio 2.5 (DS2.5) software (BIOVA, Anaheim, USA). The model with the best score was then minimized by 5000 steps of steepest descent and 2000 steps of conjugate gradient. Finally, the ProCheck procedure was used to verify the quality of the model.

Molecular docking

The optimized PAC1-R 3D structure acquired from homology modelling was selected as the initial conformation for the docking study. The binding sites were defined according to the complex structure of PAC1-EC1 and PACAP(6–38) (PDB ID: 2JOD). The preprocessing of the PAC1-R 3D structure was implemented using DS2.5, such as hydrogenation and applying CHARMm Forcefield (version 35b1) without CMAP backbone corrections. The 3D structures of small molecular chemicals, including doxycycline and SPAM1, were sketched in DS2.5, and the structure data files were stored following energy minimization. The docking procedure was implemented using the LibDock program of the DS simulation software package. LigScore1, LigScore2, PLP1, PLP2, Jain, PMF and PMF04 were used to score the binding affinity. PyMol 1.5 (Schrödinger LLC, Portland, USA) was used for visual inspection of the results and the graphical representations.

Docking analysis using Schrödinger software

The Schördinger Maestro package was employed to perform dock analysis. The 2D structures of small molecular chemicals, including doxycycline and SPAM1-5, were prepared using LigPrep (Epik). The PAC1-R receptor structure was modelled as described above [15,16] and constructed following the Protein Prepare Wizard workflow in the Maestro package. All chains of the structure were used to prepare the receptor, and all water molecules above 5 angstroms around the protein were removed. The prepared structures of small molecular chemicals were flexibly docked onto the predicted binding site of PAC1-R using Glide (XP mode) with default parameters. The binding site was selected using the Grid Generation procedure, and the docking grid was generated around the small molecular chemical (15 Å). Finally, several docking poses were obtained for the molecules, and the one with the best Glide score was chosen.

Filtration and preprocessing of small-molecule libraries for virtual screening

Virtual screening was carried out using a small-molecule library (including over 2 million small molecules) provided by TargetMol (Target Molecule Corp, Boston, USA.). First, we removed the molecules that include the PAINS structure referring to the parent nucleus of a series of chemical structures and the molecules including those parent nuclei, which can affect many assays without real binding and lead to false positive results in virtual screening [17]. The remaining molecules for docking analysis were over 1.8 million. The 2D structures of the remaining molecules were prepared using Lig-Prep (Epik) of the Maestro package. Then, the small-molecule files were finally generated for docking analysis utilizing Schrödinger software as mentioned above.

Virtual screening using Glide

First, virtual screening with the 1.8 + million small molecules from the above filtration was performed utilizing Glide at general (SP) precision; then, the top 2000 molecules were selected according to the docking score. Next, these selected molecules were further screened at extra (XP) precision utilizing Glide. The detailed number and docking results are shown in the Supplementary Data. The top five small molecules were named as small positive allosteric

modulator (SPAM) 1–5 and subject to subsequent cell experimental screening.

Cell viability assay

Cell viability was assessed by MTT assay. In brief, SH-SY5Y cells were plated into a 96-well plate at a density of 1×10^4 cells/well and incubated with or without SPAMs or DOX at concentrations ranging from 1 μM to 100 μM for 2 h before MPP + (8 mM) exposure. The PAC1-R antagonist PACAP(6–38) was used at 100 nM to detect whether the activities of SPAMs and DOX are mediated by PAC1-R. Twenty four hours after MPP + exposure, 40 μL of MTT solution (0.5 mg/mL) was added to each well after the medium was discarded. After incubation for 4 h, 100 μL isopropanol was added to each well to dissolve the formazan formed by the viable cells. The number of viable cells was determined based on the OD_{570} value of the solution. The viability of MPP + treated cells was plotted as a percentage of the OD_{570} value of control cells (without MPP + treatment; expressed as 100% viability). All experiments were performed at least three times with four parallel replicates.

Caspase-3 activity analysis

Caspase-3 activity was determined using a Caspase-3 assay kit (Beyotime Institute of Biotechnology, Shanghai, China) according to the manufacturer's instructions. Briefly, cells were lysed and centrifuged to obtain supernatants, which were mixed with buffer containing the substrate peptides for caspase-3 attached to p-nitroanilide and incubated for 2 h at 37°C. The absorbance at 405 nm (OD_{405}) was measured using a microplate reader. Caspase-3 activity was normalized by the protein concentration in the supernatant quantified using a BCA protein assay kit (Beyotime Institute of Biotechnology). All experiments were performed at least three times with four parallel replicates.

ELISA of cellular dopamine and dopamine transporter

SH-SY5Y cells were plated into a 12-well plate at a density of 1×10^5 cells/well and incubated with or without SPAMs or DOX at concentrations ranging from 1 μM to 100 μM for 2 h before MPP + (8 mM) exposure. Dopamine (DA) and dopamine transporter (DAT) concentrations in SH-SY5Y cells were measured 2 h following the addition of MPP + (8 mM) using DA and DAT ELISA kits (Enzyme-linked Biotechnology, Shanghai, China). The DA and DAT levels were further normalized by the protein concentration quantified using a BCA protein assay kit. The data were plotted as the percentage of the MPP + treated cells to the control cells (without MPP + treatment). All experiments were performed at least three times with four parallel replicates.

Terminal deoxynucleotidyl transferase dUTP nick end labelling (TUNEL) assay

SH-SY5Y cells were incubated with or without 100 μM SPAM1 or DOX for 2 h before MPP + (8 mM) exposure. Cell apoptosis was measured using a TUNEL cell apoptosis detection kit (KeyGEN Biotech, Nanjing, China) 24 h after MPP + (8 mM) exposure. The cells were observed and photographed under a microscope following treatment with DAB reagent. The mean intensity of TUNEL staining in SH-SY5Y cells was determined by Image-Pro Plus and plotted as the fold changes of the MPP + treated cells relative to the control cells (without MPP + treatment). All experiments were performed at least three times with four parallel replicates.

Isothermal titration calorimetry (ITC) assay

ITC experiments were carried out using a MicroCal iTC200 instrument (MicroCal, Northampton, USA). The recombinant PAC1-EC1 protein was prepared following the method reported previously [18]. Both recombinant PAC1-EC1 protein and peptides were dissolved in Tris buffer (20 mM Tris-HCl and 100 mM NaCl) containing 5% DMSO. The syringe was filled with SPAM1 or DOX solution, whereas PAC1-EC1 was in the cell. The 100 μL chemical solutions at a concentration of 200 μM were titrated into 280 μL of 30 μM PAC1-EC1. Titrations were performed at 25.0 ± 0.2°C. The power reference was 5 μcal/s, and the stirring rate was 750 rpm to ensure rapid mixing. The volume was 2 μL per injection, and the interval between injections was 100 s to warrant equilibrium at each titration point. Each titration was composed of 18 independent titrant additions. Background titrations were performed with chemicals in Tris buffer without the PAC1-EC1 protein and in Tris buffer with PAC1-EC1 protein but without SPAM1 or DOX. The binding isotherm was obtained by plotting the reaction heat vs. the molar ratio of each peptide to PAC1-EC1 protein. Origin 7.0 software from MicroCal was used for data analysis to obtain the binding indexes associated with the interaction events, such as the association constant (*Ka*) and entropy value (ΔH).

Antibiotic activity assay

The antibacterial effects of SPAM1 and DOX were measured by the filter paper method [19]. Circular filter papers with a diameter of 0.5 cm were prepared and sterilized for later use. The *E. coli* DH5α bacterial suspension (150 μL) was planked evenly on the solid LB medium of the plate. Each filter paper was soaked with 200 μL of SPAM1 or DOX at concentrations of 1 μM, 10 μM, and 100 μM and pasted on the bacteria-containing solid LB medium. DMSO (200 μL) was used as a control. After the plates were incubated at 37°C for 24 h, the diameter of the inhibition zone was measured, and the result was the average of three replicates.

Animals and drug treatment

Male C57/BL6 mice (8 weeks old, weight of 22–25 g) from Pengyue Experimental Animal Breeding Co. Ltd (Jinan, China) were maintained on a 12:12 h light:dark cycle at 24 ± 1°C and 55% ± 5% humidity with free access to food and water. The treatment procedure is shown in the upper part of Figure 5. In brief, at first, mice were randomly divided into six groups and injected with drugs including SPAM1 or DOX or PACAP38 or saline into the skin of neck for 7 days; then intraperitoneal (i.p.) injection of MPTP (25 mg/kg/day) was performed at 1 h following the drug injection for 14 days. The six groups were as follows: (1) normal control group (NOR): saline without MPTP, (2) MPTP group: saline + MPTP, (3) L-SMAP1 group: SPAM1 (10 μmol/kg/day) + MPTP, (4) H-SMAP1 group: SPAM1 (100 μmol/kg/day) + MPTP, (5) DOX group: DOX (100 μmol/kg/day) + MPTP, and (6) PACAP38 group: PACAP38 (100 nmol/kg/day) + MPTP.

Pole-climbing test

The pole-climbing test is a method used to measure motor coordination and balance in mouse models of PD. The apparatus for the pole-climbing test is a 50 cm high, gauze-taped (diameter, 1 cm) pole. On the 21st day, 2 h after the last i.p. injection of MPTP, the pole-climbing test was conducted. The time spent by each mouse to complete turning orientation (T-turn) and the time spent to com-

plete both turning orientation and descending the pole (T-total) were counted. Meanwhile, the tests were recorded via an overhead digital video camera, and the results were plotted as the average T-turn time and the average T-total time from three repeated tests.

Paw suspension test

The apparatus for the paw suspension test is a horizontal metal wire with a l mm diameter placed at a height of 30 cm above the ground. On the 21st day, the paw suspension test was conducted 2 h after the last i.p. injection of MPTP. Each mouse was graded with a score according to its performance. The mice which are able to grasp the metal wire with 2 front paws received a score of three, those which are able to grasp the metal wire with 1 front paw received a score of two, those which struggled but could not grasp the metal wire with either front paw received a score of one, and those which dropped directly without any grasp received a score of zero. The results were plotted as average scores from three repeated tests.

Open field test

The open field (OF) test was performed on the 21st day 2 h after the last i.p. injection of MPTP. The OF test was conducted using a square box (30 cm × 30 cm × 30 cm) made of gray Plexiglass plastic. Individually, the mouse was placed in the center of the OF and allowed to freely explore for 5 min while being recorded. The OF was cleaned thoroughly between each mouse to eliminate excretions and any odor cues using 70% ethanol and allowed to air dry. The FIJI/ImageJ Plugin Mouse Behavioral Analysis Toolbox (MouBeAT) software (version 1.00) was used to analyze the videos. Locomotor activity was determined by the total distance travelled and average speed of the mice, as calculated by MouBeAt. Exploratory behavior was defined as the number of times a mouse entered the center of the OF and the time spent in the center.

Tissue preparation

After motor function tests were finished, mice were euthanized and the brain tissues were quickly removed and cleaned with cold 0.9% saline. Then, the striatum and other brain tissues were dissected and immediately frozen at −80°C for subsequent analysis. Brain tissue samples were thawed and homogenized in cold 0.9% saline.

Measurement of striatal DA, DOPAC and HVA levels

The levels of DA, DOPAC and HVA in the striatum were measured by HPLC-LC/MS. Briefly, the striatum samples were weighed, thawed to room temperature and homogenized in methanol. The homogenate of each sample was centrifuged at 10,000 *g* for 10 min at 4°C. The supernatant was filtered through a 0.22 μm filter membrane, and 10 μL of the filtrate was subject to analysis using an HPLC-LC/MS system consisting of an Agilent 1260 Infinity (Agilent Technologies, Palo Alto, USA) and an AB Sciex 4000 QTRAP® triple quadrupole mass spectrometer (AB Sciex, Concord, Canada). The analytical column used was a Poroshell 120 EC-C18 (4.6 × 50 mm, 2.7 μm).

Antioxidative activity evaluation

After the excision of the striatum, brain tissue was homogenized in ice-cold saline with a tissue homogenizer. The whole-brain tissue homogenate without the striatum was centrifuged at 3000 *g* for 10 min, and the supernatant was subject to measurement of superoxide dismutase (SOD) activity and malondialdehyde (MDA) level using the SOD kit and MDA kit (Jiancheng Biotechnology) respectively according to the manufacturer's instructions. All the antioxidative data were normalized by the protein concentration of the supernatant quantified using a BCA protein assay kit (Beyotime Institute of Biotechnology). All experiments were performed at least three times with four parallel replicates.

Immunohistochemical analysis

Brain tissue samples of the substantia nigra and striatum were fixed in 4% paraformaldehyde at 4°C for 48 h before dehydration and embedding in paraffin. Next, 5-μm thick coronal sections were cut with a microtome and mounted on glass slides. The sections were deparaffinized in xylene and rehydrated through decreasing concentrations of ethanol. A polyclonal antibody against human PAC1-R/ADCYAP1R1 506-525aa (ab28670; Abcam, Cambridge, UK) was used to detect PAC1-R. An ABC Elite kit (Vecter Lab., Burlingame, USA) was used for immunohistochemical staining. PAC1-R-positive cells were made visible with 3,3'-diaminoben-zidine tetrahydrochloride, and the tissue sections were counterstained with hematoxylin. ImageJ was used for the semi-quantification of DAB-positive cells normalized to the nuclei (hematoxylin stain).

Western blot analysis

Total proteins were extracted from the corpus striatum samples using RIPA buffer (50 mM Tris-HCl, pH 7.4, 150 mM NaCl, 20 mM EDTA, 1% Triton X-100, 1% sodium deoxycholate, 1% SDS and protease inhibitors (Beyotime Institute of Biotechnology) on ice for 30 min, separated by SDS-PAGE, and blotted onto PVDF membranes. Membranes were incubated with rabbit polyclonal antibody against human PAC1-R/ADCYAP1R1 506-525aa (Abcam) and anti-β-actin antibody (ab227387; Abcam), followed by incubation with HRP-conjugated anti-rabbit IgG secondary antibody. Immunocomplexes were visualized through chemiluminescence using an ECL kit (Beyotime Institute of Biotechnology).

Statistical analysis

Statistical analysis was performed with GraphPad Prism 8. Data are presented as the mean ± standard error of the mean (SEM). One-way analysis of variance (ANOVA) was used to evaluate the differences among groups. Differences with $P < 0.05$ were considered to be statistically significant.

Results

Computer virtual screening of SPAM1

First, the Schördinger Maestro package was employed to perform dock analysis of DOX with PAC1-R, and the binding details overlapped with the molecular docking result utilizing DS2.5 software. As shown in Figure 1A (left), the conformations of DOX docked using Schrödinger software (blue stick) and DS software (yellow stick) are almost in the same location. Simultaneously, the binding mode (Figure 1A, right) illustrated the same interactions that exist between DOX and key residues of PAC1-R, including ASP111, ILE61, ASP116, PHE27 and PHE115, as described previously [15,16].

Virtual screening was carried out using a small-molecule library (including over 2 million small molecules) provided by TargetMol. After two-level precision screening with Glide, five chemicals with the predicted affinities listed at the top of docking results (Supplementary Data) were selected and named SPAM1–5, which are listed

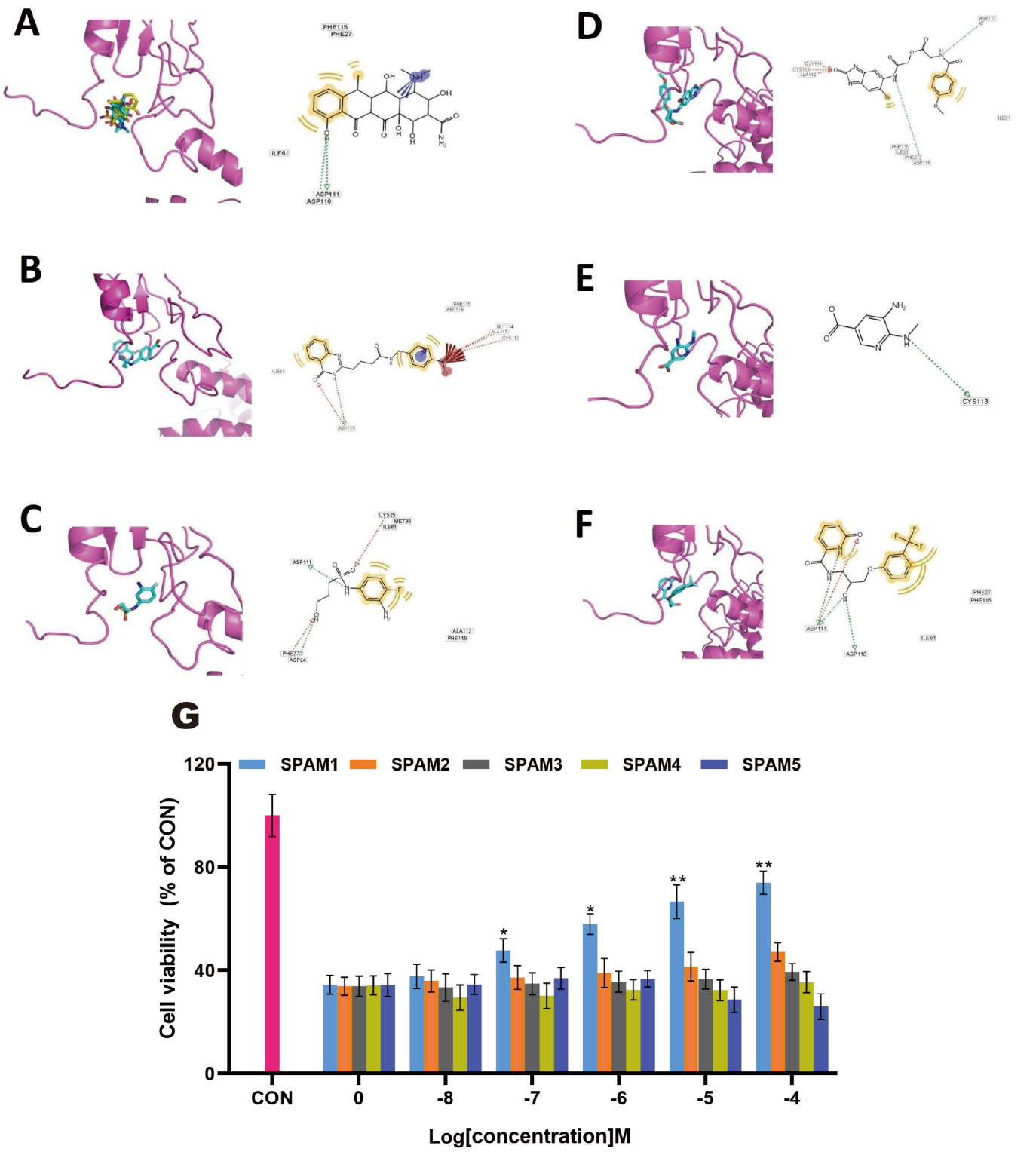

Figure 1. The binding sites and the details of predicted binding modes of DOX and SPAM1–5 and the cytoprotective activity screening of SPAM1–5 (A–F) The protein PAC1-R is shown as a cartoon, and the molecule is shown as sticks. The blue stick illustrates the docked DOX using Schrödinger software, and the yellow stick is the DOX using DS software. The contact residues are shown and labelled by type and number. The red/green dotted line illustrates the hydrogen bond interaction. (G) Cell viability assayed by MTT showed that only SPAM1 at concentrations from 1 μM to 100 μM had a significant cytoprotective effect. $*P<0.05$, $**P<0.01$. Data are presented as the mean ± SEM of three experiments.

in Table 1. The binding sites and the details of the predicted binding mode of SPAM1–5 are shown in Figure 1B–F.

Neuroprotective activity screening of SPAM1 with MPP+ PD cell model

The five candidates SPAM1-5 with top affinities with PAC1-R from virtual screening were subject to cytoprotective activity screening by measuring their protective activities against the apoptosis induced by MPP+ in SH-SY5Y cells. As shown in Figure 1G, MTT assay results indicated that SPAM1 (1–100 μM) significantly increased the cell viability decreased by MPP+ ($P < 0.01$, vs MPP+), and the cytoprotective activity of SPAM1 was increased in a concentration-dependent manner.

When the cytoprotective activity of SPAM1 was compared with DOX, as shown in Figure 2A, SPAM1 (100 μM) had a significantly stronger cytoprotective effect than DOX (100 μM) ($P < 0.05$, SPAM1 vs DOX). Furthermore, the cytoprotective effects of SPAM1 and DOX were both inhibited by the PAC1-R antagonist PACAP(6–38) [$P < 0.05$, vs + PACAP(6–38)], indicating that the cytoprotective activities of SPAM1 and DOX are both mediated by PAC1-R.

The assay results of caspase 3 activity (Figure 2B), DA (Figure 2C) and DAT (Figure 2D) contents showed that both SPAM1 and DOX at concentrations of 10 μM–100 μM had significant positive effects against MPP+ in SH-SY5Y cells by inhibiting caspase 3 activity and increasing DA and DAT contents, and SPAM1 at 100 μM showed significantly stronger effects than 100 μM DOX ($P < 0.05$, SPAM1 vs

Table 1. List of five chemicals with the top highest affinities in the virtual screening results targeting the positive allosteric binding site of PAC1-R

Name	Title	Structure	Full name	Docking score
SPAM1	Enamine_Z71395360	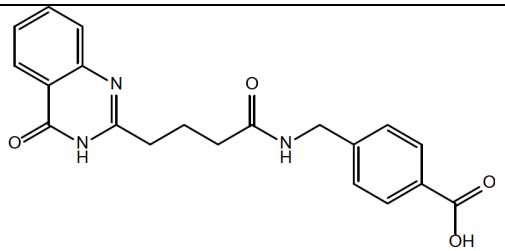	4-((4-(4-oxo-3,4-dihydroquinazolin-2-yl)butanamido) methyl)benzoic acid	−8.178
SPAM2	Enamine_Z594413782	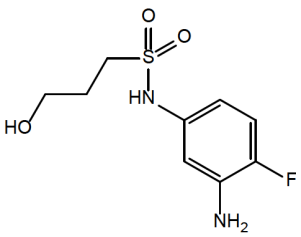	N-(3-amino-4-fluorophenyl)-3-hydroxypropane-1-sulfonamide	−8.032
SPAM3	Enamine_Z87576051	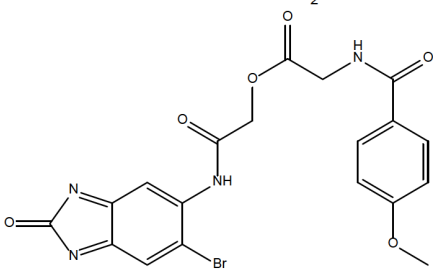	2-((6-bromo-2-oxo-2H-benzo[d]imidazol-5-yl)amino)-2-oxoethyl (4-methoxybenzoyl)glycinate	−7.762
SPAM4	Enamine_Z1762997274	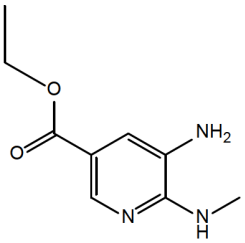	Ethyl 5-amino-6-(methylamino)nicotinate	−7.667
SPAM5	Enamine_Z1916181887	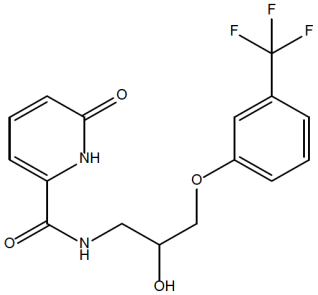	N-(2-hydroxy-3-(3-(trifluoromethyl)phenoxy)propyl)-6-oxo-1,6-dihydropyridine-2-carboxamide	−7.646

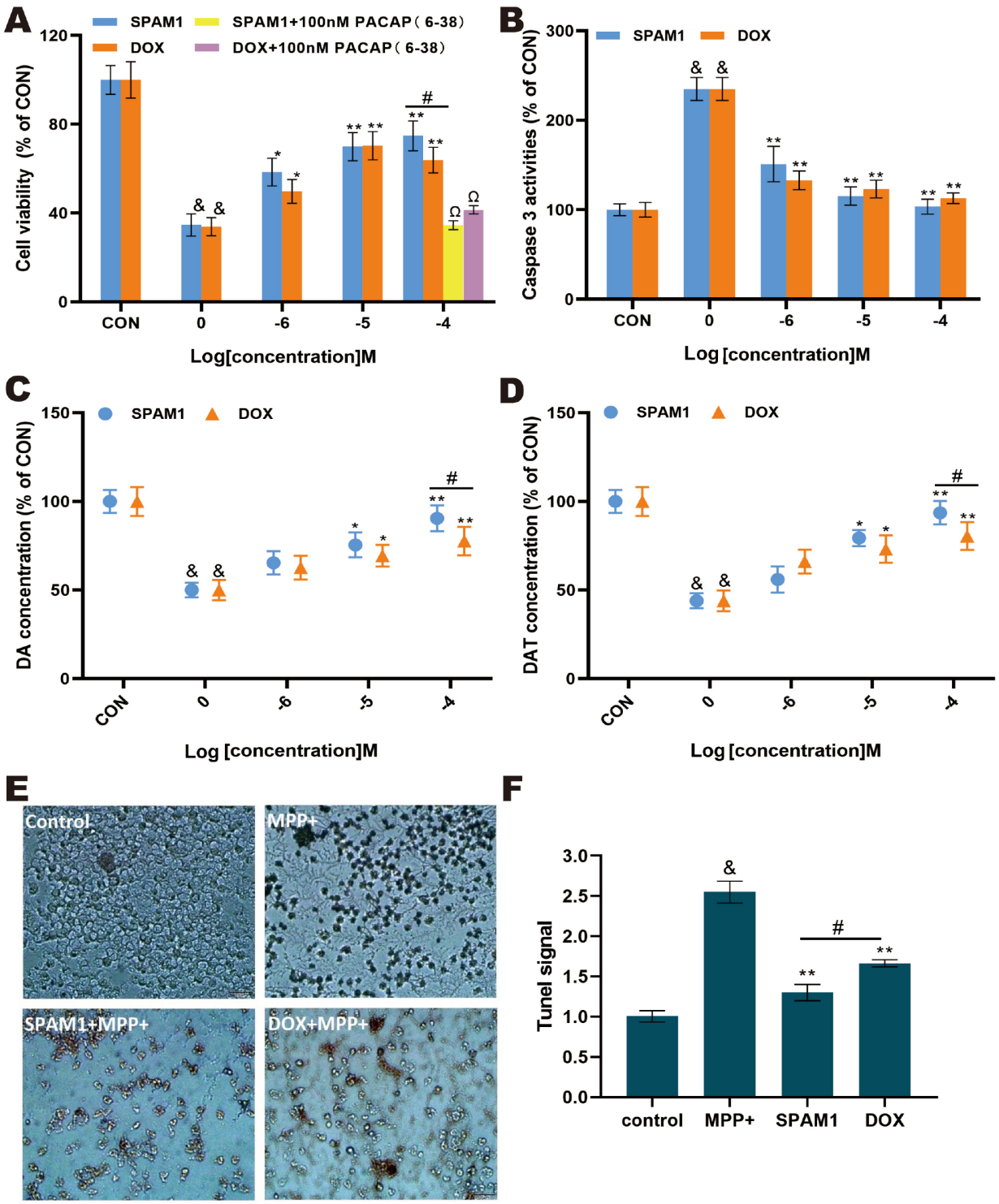

Figure 2. Cell viability, caspase 3 activity, DA levels, DAT levels and TUNEL assay in MPP+ induced SH-SY5Y cells of PD model (A) The MTT assay showed that both SPAM1 and DOX at concentrations from 1 to 100 μM significantly increased the cell viability decreased by MPP + treatment, and SPAM1 (100 μM) had a significantly stronger cytoprotective effect than DOX (100 μM). Meanwhile, the cytoprotective effects of SPAM1 (100 μM) and DOX (100 μM) were both inhibited significantly by PACAP(6–38) (100 nM). (B) The results of caspase 3 activity showed that both SPAM1 and DOX at concentrations from 1 to 100 μM had significant protective effects against the damaging effects of MPP + by decreasing caspase 3 activity. (C,D) The results of DA and DAT levels showed that both SPAM1 and DOX at concentrations from 10 to 100 μM had significant protective effects against the damaging effects of MPP + by increasing DA and DAT contents, and SPAM1 at 100 μM showed significantly stronger effects than DOX (100 μM). (E,F) Effects of SPAM1 (100 μM) and DOX (100 μM) on apoptosis determined by TUNEL assay in SH-SY5Y cells induced by MPP + and the corresponding quantitative analysis of the TUNEL images. SPAM1 (100 μM) had significantly stronger anti-apoptotic activity than DOX (100 μM). $^{\&}P < 0.05$, MPP + group vs control group; $^{*}P < 0.05$, vs MPP + group; $^{**}P < 0.01$, vs MPP + group; $^{\#}P < 0.05$, SPAM1 vs DOX; $^{\Omega}P < 0.05$, vs + PACAP(6–38). Data are presented as the mean ± SEM of three experiments. Scale bar = 100 μm.

DOX) in inducing DA and DAT contents.

The TUNEL assay results, including microscope images and corresponding quantitative analysis (Figure 2E,F), showed that MPP+ treatment increased the number of cells stained in the TUNEL assay, and treatment with SPAM1 (100 μM) or DOX (100 μM) significantly reduced the TUNEL signal, confirming the cytoprotective activities of SPAM1 and DOX against the apoptosis induced by MPP+ in SH-SY5Y cells, while the anti-apoptotic activity of SPAM1 (100 μM) was much stronger than that of DOX (100 μM) ($P < 0.05$, SPAM1 vs DOX).

Binding affinity and antibiotic activity of SPAM1 and DOX

To confirm the advantage of SPAM1, we further compared the binding details and binding affinities of SPAM1 and DOX targeting PAC1-R with DS software. As shown in Figure 3, two hydrogen bonds are formed between DOX and ASP116. In addition, DOX also has hydrophobic interactions with CYS25, PHE27, ASN60, ASP111, GLY114, PHE115 and PHE110. SPAM1 also forms two hydrogen bonds with the carboxyl group of ASP116 and forms one hydrogen bond with GLY 114 and ASP 124. In addition, SPAM1 forms π-π water transport interaction with PHE27 and PHE115. In a word, the molecular docking with DS software showed that the theoretical affinity of SPAM1 with PAC1-R is higher than the affinity of DOX (Table 2).

Furthermore, molecular docking (Figure 3) showed that the binding site and the binding details of SPAM1 with the N-terminal extracellular domain of PAC1-R are different from those of DOX binding to PAC1-R. The residues SER120, GLY123 and ASP124 are involved in the interaction of SPAM1 with PAC1-R but do not contribute to the interaction of DOX with PAC1-R. These differences indicated that (1) SPAM1 has a slightly larger binding site than DOX, and PACAP(30–37) bind with PAC1-R, which is closer to the binding site recognized by PACAP(28–38); and (2) the affinity of SPAM1 to PAC1-R should be higher than the affinity of DOX because the more the interacting residues the higher the structural fitness.

The subsequent affinity assay using isothermal titration calorimetry (ITC) (Figure 4A–C) confirmed that SPAM1 binds with the PAC1-EC1 protein with an association constant (Ka) value of $2.59 \times 10^6 \pm 4.87 \times 10^5$ M^{-1}, which is significantly higher than DOX with Ka = $1.03 \times 10^6 \pm 2.44 \times 10^5$ M^{-1}. The reaction heat released by the titration of SPAM1 is ΔH = −6157 ± 603.5 cal/mol, much larger than the heat released by the titration of DOX with ΔH of −5478 ± 253.4 cal/mol. These data confirmed that SPAM1 has a higher affinity for PAC1-R than DOX, which may be the reason why

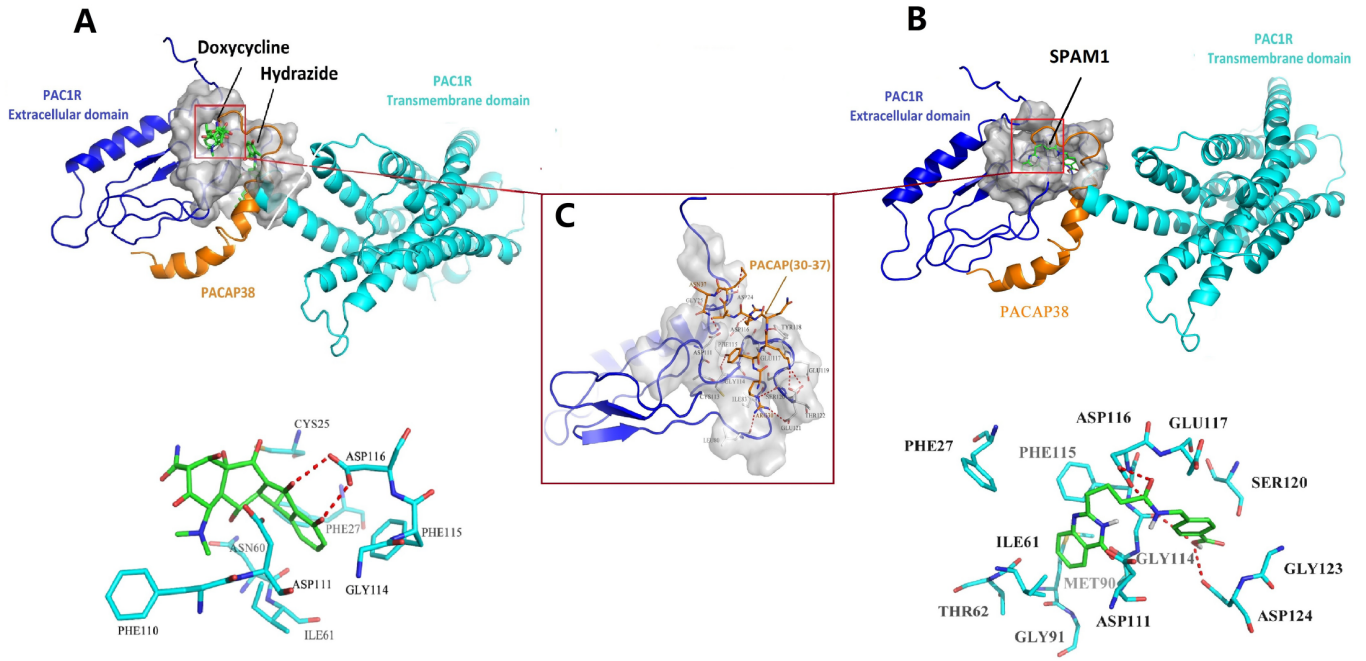

Figure 3. Molecular docking and details of the predicted binding mode of DOX and SPAM1 targeting PAC1-R (A) The predicted binding site of DOX to the N-terminal extracellular domain of PAC1-R is different from the binding site of hydrazide as an antagonist of PAC1-R. (B) The predicted binding site of SPAM1 targeting PAC1-R involves the site recognized by DOX, but the binding site of SPAM1 was slightly larger than that recognized by DOX. As shown in the predicted binding modes (lower), SER120, GLY123 and ASP124 are involved in the interaction of SPAM1 with PAC1-R but are not included in the residues mediating the binding of DOX with PAC1-R. PAC1 and PACAP(6–38) are shown as cartoon styles, and the chemicals are shown as sticks. The binding site was represented by surface modelling. Dark blue represents the N-terminal extracellular domain of PAC1, light blue corresponds to the transmembrane domain of PAC1-R, orange corresponds to PACAP(6–38), and green represents DOX and SPAM1. The contacting residues are labelled by type and numbers, and the red dotted line illustrates the hydrogen bond interactions. (C) Both the predicted binding site of DOX and SPAM1 to the N-terminal extracellular domain of PAC1-R is similar to the binding site of PACAP(30–37).

Table 2. The binding affinities of SPAM1 and DOX with PAC1-R predicted by computer molecular docking using DS software

Scoring function	LigScore1	LigScore2	−PLP1	−PLP2
SPAM1	4.68*	4.18*	93.22*	91.9*
DOX	1.88	3.59	54.24	47.51

*Higher score means higher theoretical affinity.

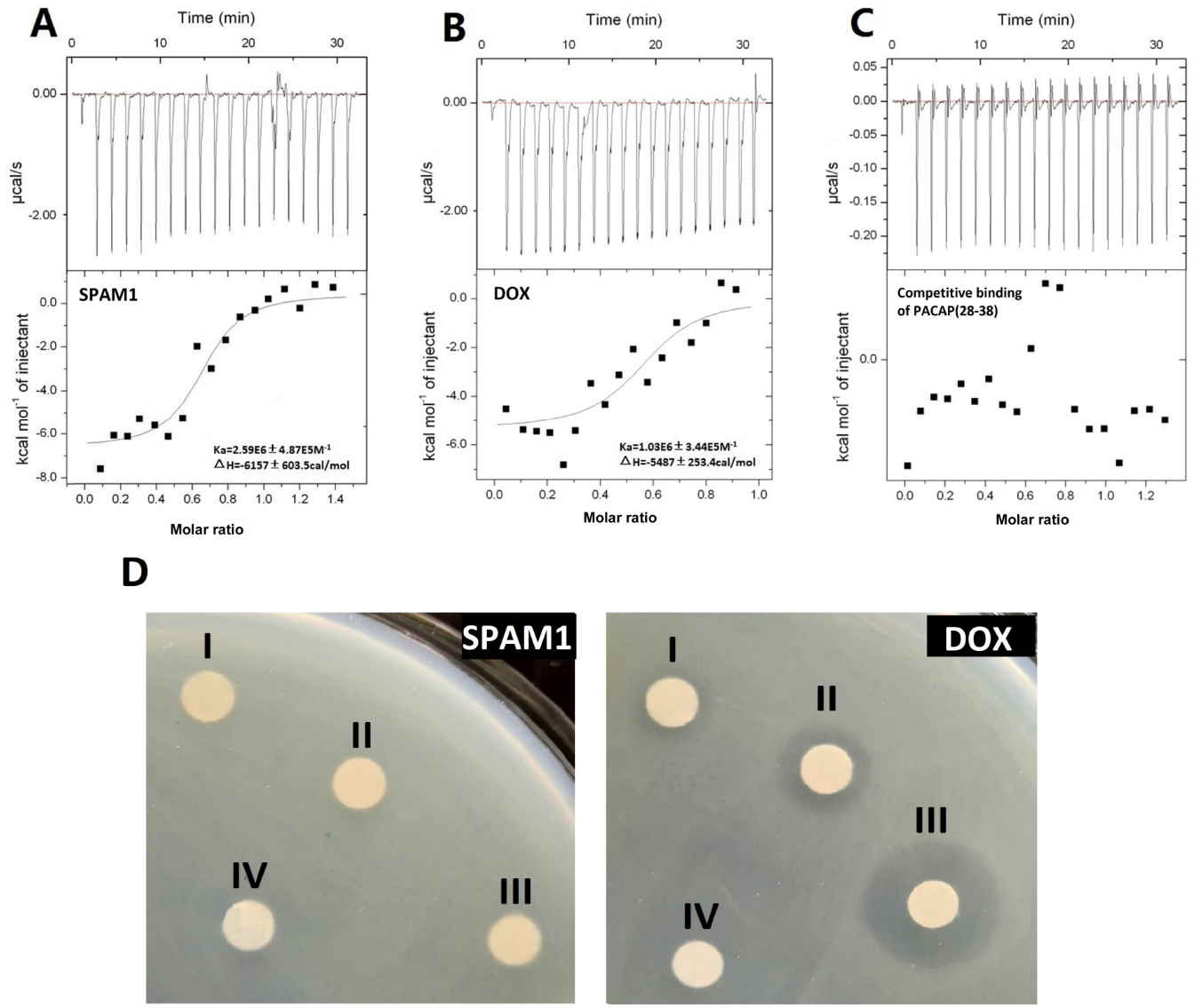

Figure 4. Affinities of SPAM1, DOX and competitive binding of PACAP(28–38) with recombinant PAC1-EC1 protein measured by ITC assay and the antibiotic assay of SPAM1 and DOX (A–C) The thermogram is shown in the upper panel, and the binding isotherm obtained by plotting the reaction heat vs the molar ratio of each chemical to PAC1-EC1 protein is shown in the lower panel. (D) The antibiotic assay of SPAM1 (left) and DOX (right). Small round pieces of paper with a diameter of 0.5 cm soaked with 200 μL of SPAM1 or DOX at concentrations of 1 μM (I), 10 μM (II) and 100 μM (III) were placed on LB agarose after the suspension of *E. coli* DH5α was planked, and dimethylsulfoxide (DMSO) (IV) was used as a control. After incubation at 37°C for 24 h, there was no observable antibacterial circle surrounding the paper pieces with SPAM1 at any detected concentration and DMSO, while there was a significant antibacterial circle surrounding the paper pieces with DOX, and the antibacterial circle enlarged with increasing DOX concentration. Data are presented as the mean ± SEM, $n = 3$.

SPAM1 has significantly stronger antiapoptotic activity than DOX. Furthermore, when PAC1-EC1 was presaturated with PACAP(28–38) (100 nM), no binding signal was detected from the titration of SPAM1 (Figure 4C), indicating that the site recognized by SPAM1 in PAC1-EC1 is overlapped by PACAP(28–38), which is consistent with the theoretical molecular docking result shown in Figure 3.

The antibiotic activity of DOX has been considered a side effect that cannot be ignored, which will hinder its extensive clinical use, so we detected the antibiotic activity of SPAM1. As shown in Figure 4D, the antibacterial circles surrounding the paper pieces with DOX extended in a concentration-dependent manner from 1 μM to 100 μM, while there was no significant viable antibacterial circle surrounding the paper pieces with SPAM1 at concentrations of 1 μM-100 μM, indicating that SPAM1 has no significant antibiotic activity. The lack of antibiotic activity of SPAM1 suggests that SPAM1 may exert more positive effects *in vivo* than DOX.

Neuroprotective activity confirmation of SPAM1 *in vivo* with the MPTP PD mouse model

As shown in Figure 5, intraperitoneal injection of MPTP alone, low-dose SPAM1 (10 μmol/kg/day) + MPTP (L-SPAM1), high-dose SPAM1 (100 μmol/kg/day) + MPTP (H-SPAM1), DOX (100 μmol/kg/day) + MPTP, and PACAP38 (100 nmol/kg/day) + MPTP did not produce a significant body weight decrease compared to the normal control (NOR) (Figure 5A). Compared to the control group, the suspension score of the MPTP group was sig-

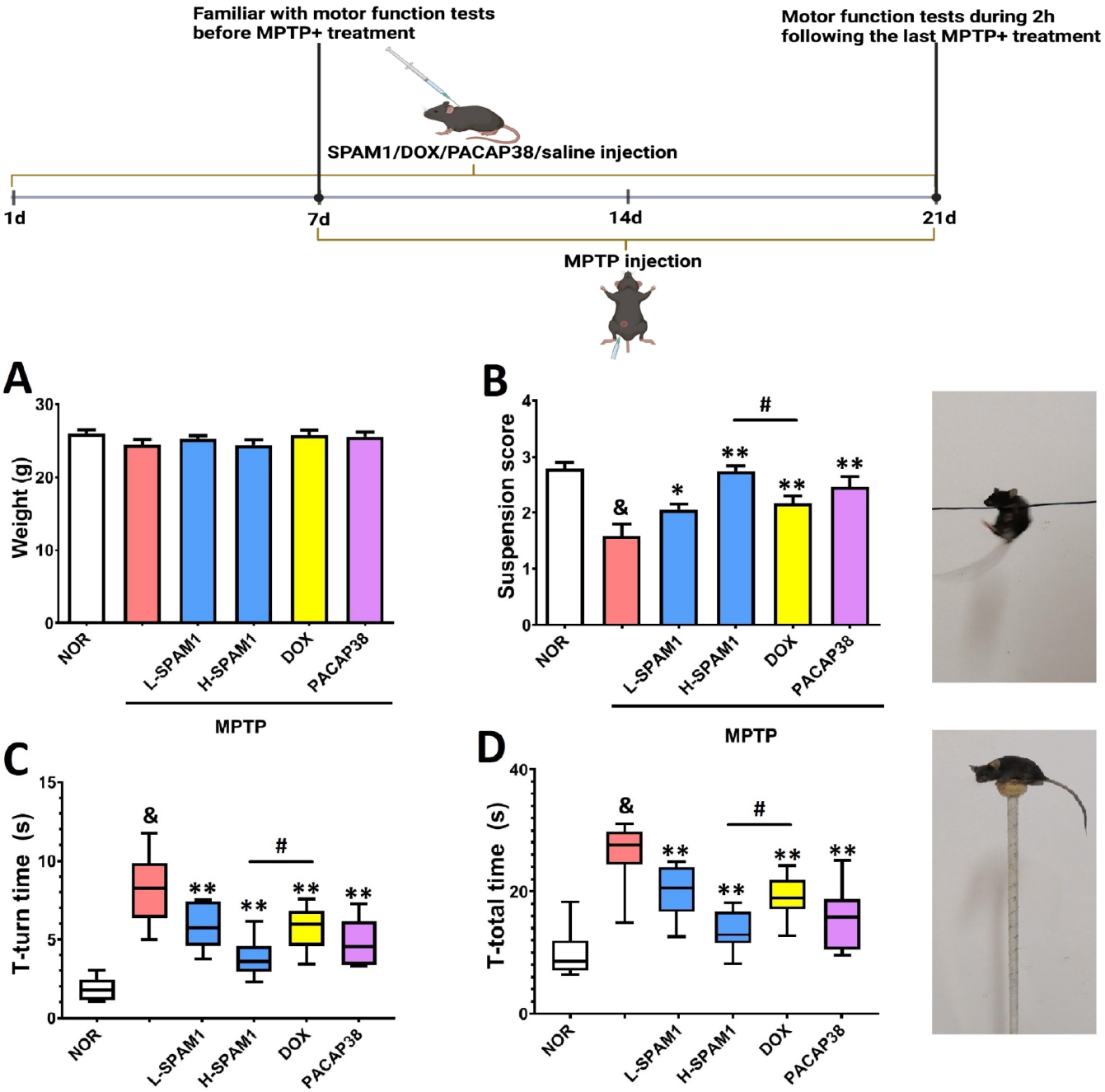

Figure 5. Effects of SPAM1 at a low dose, named L-SPAM1, SPAM1 at a high dose, named H-SPAM1, DOX and PACAP38, on MPTP-induced motor function impairment The animal MPTP PD model and the treatment procedure are shown in the upper panel. (A) Treatment with chemicals and MPTP did not significantly affect mouse body weight. (B) The paw suspension score showed that L-SPAM1, H-SPAM1, DOX and PACAP38 protected mice from the impairment of MPTP on motor functions, while treatment with H-SPAM1 showed a significantly more efficient protective effect than DOX at the same concentration of 100 μmol/kg/day. The average time to complete the T-turn (C) and the average time to complete both the T-turn and descending (T-total) (D) also showed that DOX displayed a weaker protective effect against MPTP-induced motor impairment than H-SPAM1. $^{\&}P<0.05$, MPTP group vs control group (NOR); $^{*}P<0.05$, vs MPTP group; $^{**}P<0.01$, vs MPTP group; $^{\#}P<0.05$, DOX vs H-SPAM1. Data are presented as the mean ± SEM, $n\geq10$. The paw suspension test and the pole-climbing test are shown on the right.

nificantly decreased (Figure 5B); the T-turn time (Figure 5C) and T-total time (Figure 5D) were significantly increased ($P<0.05$ MPTP vs NOR), indicating that the motor function was significantly impaired by treatment with MPTP. The results of motor function assays indicated the following: (1) Treatment with SPAM1 at both low and high doses improves the motor function impaired by MPTP, while SPAM1 at high doses has more effective neuroprotective activity than SPAM1 at low doses, suggesting that SPAM1 works in a concentration-dependent manner *in vivo*. (2) Treatment with DOX and PACAP38 also has significant protective effects against MPTP by increasing the suspension score and decreasing the T-turn time and T-total time of the pole-climbing test, while the protective effect of DOX and PACAP38 against MPTP is weaker than that of H-SPAM1 because the group treated with DOX + MPTP or PACAP38

+ MPTP displayed a significantly lower suspension score and longer T-turn time than the group treated with H-SPAM1 + MPTP ($P < 0.05$, DOX vs H-SPAM1).

Further experiments confirmed that administration of MPTP induced a marked decrease in the levels of DA and its metabolites, including DOPAC and HVA, in the striatum compared to the normal control group (NOR) (Figure 6A–C; $P < 0.05$ MPTP vs NOR). Treatment with L-SPAM1 significantly increased the levels of DA and HVA in the striatum, but the activity of L-SPAM1 was significantly lower than that of H-SPAM1. Both treatment with DOX and PACAP38 significantly attenuated the decrease in the levels of DA and DOPAC in the striatum induced by MPTP, while the H-SPAM1 group had significantly higher levels of DA and HVA than the DOX and PACAP38 groups ($P < 0.05$, DOX vs H-SPAM1).

The antioxidant index assay (Figure 6D,E) confirmed that MPTP treatment induced a significant decrease in SOD activity and a significant increase in MDA in the brain. Treatment with H-SPAM1 and DOX at a concentration of 100 μmol/kg/day significantly promoted SOD activity and decreased MDA level, whereas the antioxidant activity of H-SPAM1 was significantly stronger than that of DOX and PACAP38 by promoting SOD activity ($P < 0.05$, DOX vs H-SPAM1).

Figure 6F showed that L-SPAM1, H-SPAM1 and DOX have a positive tendency to reduce the caspase 3 activity increase induced by MPTP, which indicated that both SPAM1 and DOX have significant anti-apoptotic activities.

SPAM1 prevents MPTP-induced deficiency in locomotor and exploratory behavior

MPTP induced significant defects in the exploratory behavior of the mice, as determined by a reduction in the number of entries and the time spent in the center quadrant of the open field (OF) (Figure 7A–C; $P < 0.05$ MPTP vs NOR). The results of the exploratory behavior assays (Figure 7B,C) indicated the following: (1) Both L-SPAM1 and H-SPAM1 exert positive effects in improving the exploratory behavior of mice impaired by MPTP, while H-SPAM1 is significantly more effective than L-SPAM1. (2) DOX and PACAP38 also show significant positive effects against MPTP by increasing the times of entering the center and the time spent in the center, while the positive effect of DOX and PACAP38 against MPTP is weaker than that of H-SPAM1 because the group treated with DOX + MPTP and PACAP38 + MPTP displayed significantly fewer times of entering the center and the time spent in the center than the group treated with H-SPAM1 + MPTP ($P < 0.05$, DOX vs H-SPAM1).

The effects of SPAM1 on locomotor behavior were also assessed by comparing the total distance travelled (Figure 7D) and the average speed (Figure 7E). MPTP significantly impaired locomotion after 14 days of treatment with MPTP. There was a significant reduction in the total distance travelled and average speed in the saline + MPTP group (Figure 7D,E; $P < 0.05$ MPTP vs NOR). SPAM1-treatment was able to prevent defects in locomotor behavior in mice. As expected, the positive effect of DOX against MPTP was weaker than that of H-SPAM1 because the group treated with DOX + MPTP displayed significantly lower total distances and average speed than the group treated with H-SPAM1 + MPTP ($P < 0.05$, DOX vs H-SPAM1).

SPAM1 prevents the decrease of brain PAC1-R level in MPTP-treated mice

To assess whether SPAM1 exerts neuroprotective activity by upregulating PAC1-R level, we analyzed the expression level of PAC1-R in MPTP-treated mouse substantia nigra and striatum (Figure 8A) by immunohistochemical staining and in MPTP-treated mouse corpus striatum by western blot analysis (Figure 8B).

The immunohistochemical images and corresponding statistical analysis showed that MPTP administration resulted in a significant reduction in PAC1-R protein expression in the substantia nigra and striatum (Figure 8A; $P < 0.05$ MPTP vs NOR), and SPAM1 treatment significantly upregulated the expression of PAC1-R in the substantia nigra and striatum at both low and high dosages compared with the MPTP group, while H-SPAM1 had a much more positive tendency to increase the level of PAC1-R than L-SPAM1. Treatment with SPAM1, DOX or PACAP38 significantly attenuated the decrease in the levels of PAC1-R in the substantia nigra and striatum induced by MPTP.

Western blot analysis of PAC1-R in the corpus striatum showed a significant reduction in PAC1-R level in the MPTP group, which was significantly ameliorated by SPAM1 in a dose-dependent manner. Meanwhile, DOX and PACAP38 also significantly blocked the decrease in the level of PAC1-R (Figure 8B).

Discussion

In this study, we successfully identified the compound 4-{[4-(4-Oxo-3,4-2-yl)butanamido]methyl}benzoic acid ($C_{20}H_{19}N_3O_4$) (TargetMol ID: Enamine_Z71395360) (PubChem ID: 135680088) by virtual and experimental screening as a novel small molecule positive allosteric modulator (SPAM1) targeting the positive allosteric modulation site in the N-terminal extracellular domain of PAC1-R, which is also recognized by DOX [15,16].

The cell experiment data showed that SPAM1 has more effective cytoprotective activity against MPP + –induced apoptosis than DOX in SH-SY5Y cells, especially at a concentration of 100 μM. Meanwhile, SPAM1 exerts significant effective neuroprotective activity in a mouse PD model induced by MPTP by blocking motor function impairment induced by MPTP, promoting the levels of DA and its metabolites, and lowering the oxidative stress status in the brain, and the effect of SPAM1 is much stronger than that of DOX at a dose of 100 μmol/kg/day. Both the *in vitro* and *in vivo* data indicated that SPAM1 works more efficiently than DOX by targeting PAC1-R.

There are several factors contributing to the higher neuroprotective activity of SPAM1 than DOX against PD cellular and animal models. One main reason is the higher affinity of SPAM1 for PAC1-R. Both the computer predicted affinity (Table 2) and the affinity determined by ITC showed that SPAM1 targets PAC1-R with a significantly higher affinity than DOX. Furthermore, the binding details analyzed by the DS software showed that more residues, such as ASP114, are involved in the docking of SPAM1 to PAC1-EC1, indicating that the binding scope of the site bond by SPAM1 is larger than the site recognized by DOX and more similar to the binding site recognized by PACAP(28–38). Although the detailed mechanism is not very clear, PACAP(28–38) has been reported to play a significant role in enhancing the activation of PAC1-R [20] and regulating the activation of PAC1-R [21]. The more similar binding site of SPAM1 in PAC1-EC1 with the site of PACAP(28–38) than the site recognized by DOX means SPAM1 may exert a stronger effect on the activity of PAC1-R than DOX, which may be another reason why SPAM1 has more effective neuroprotective activity than DOX mediated by PAC1-R. Furthermore, unlike DOX, SPAM1 has no significant antibiotic activity, which may be another reason why

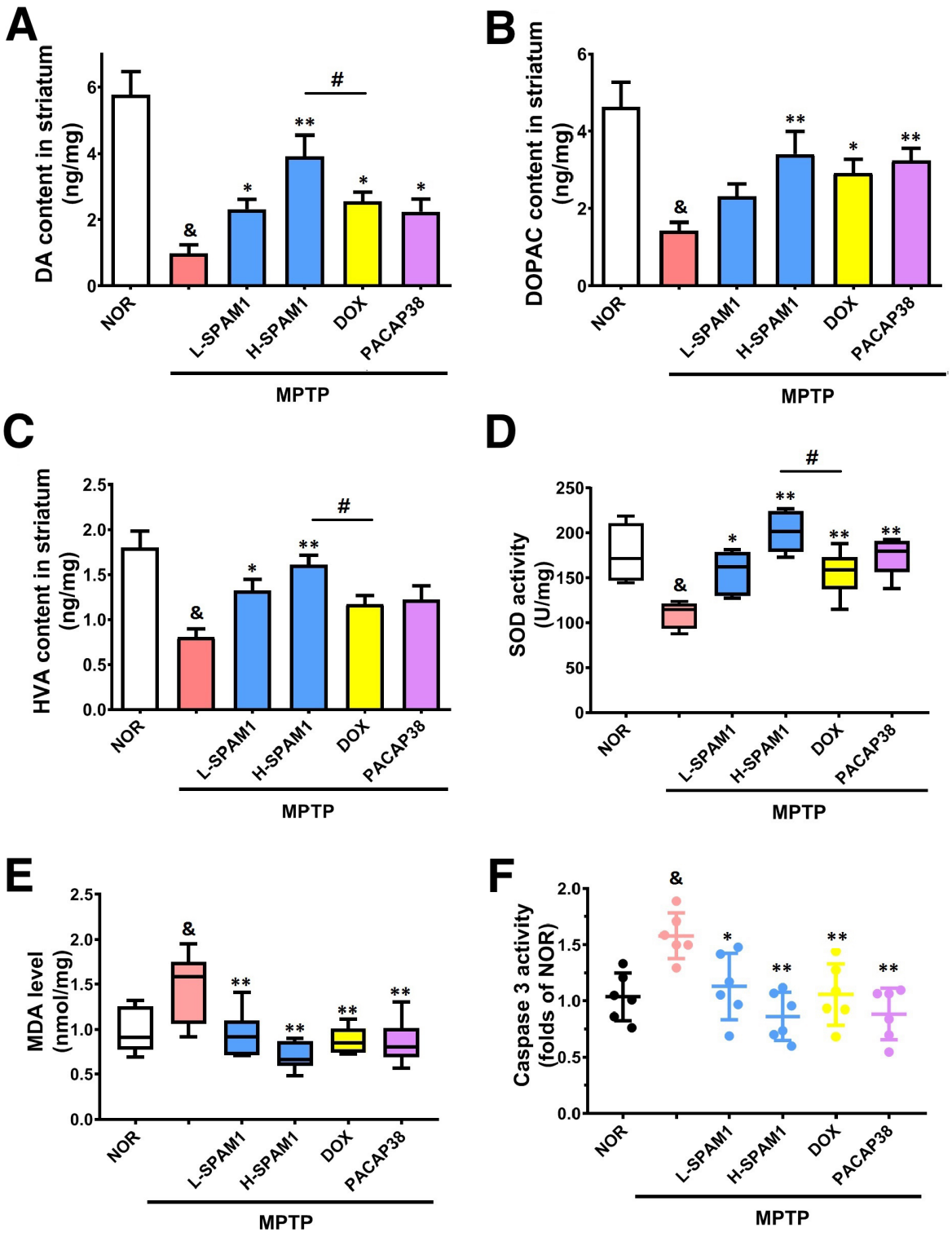

Figure 6. Effects of L-SPAM1, H-SPAM1, DOX and PACAP38 on the levels of DA, DOPAC, and HVA in the striatum and brain SOD activity, MDA levels and caspase 3 activities in MPTP-treated mice (A–C) DA, DOPAC and HVA concentrations in the striatum assayed by HPLC were significantly reduced by MPTP treatment. H-SPAM1 and DOX treatment significantly blocked the negative effect of MPTP on DA and HVA, while H-SPAM1 had significantly stronger effects than DOX. L-SPAM1 treatment significantly blocked the decrease in DA, DOPAC and HVA, but the effect of L-SPAM1 was weaker than that of H-SPAM1. (D,E) The antioxidant index assays confirmed that the SOD activity decreased and MDA level increased significantly in the brain treated with MPTP. Treatment with H-SPAM1 and DOX significantly promoted SOD activity against MPTP, while H-SPAM1 exerted a significantly more effective effect on SOD activity in the brain than DOX. (F) Brain caspase 3 activity was increased by MPTP, and SPAM1, DOX and PACAP38 significantly inhibited the increase in caspase 3 induced by MPTP. $^{\&}P < 0.05$, MPTP group vs control group (NOR); $^{*}P < 0.05$, vs MPTP group; $^{**}P < 0.01$, vs MPTP group; $^{\#}P < 0.05$, DOX vs H-SPAM1. Data are presented as the mean ± SEM, $n \geq 6$.

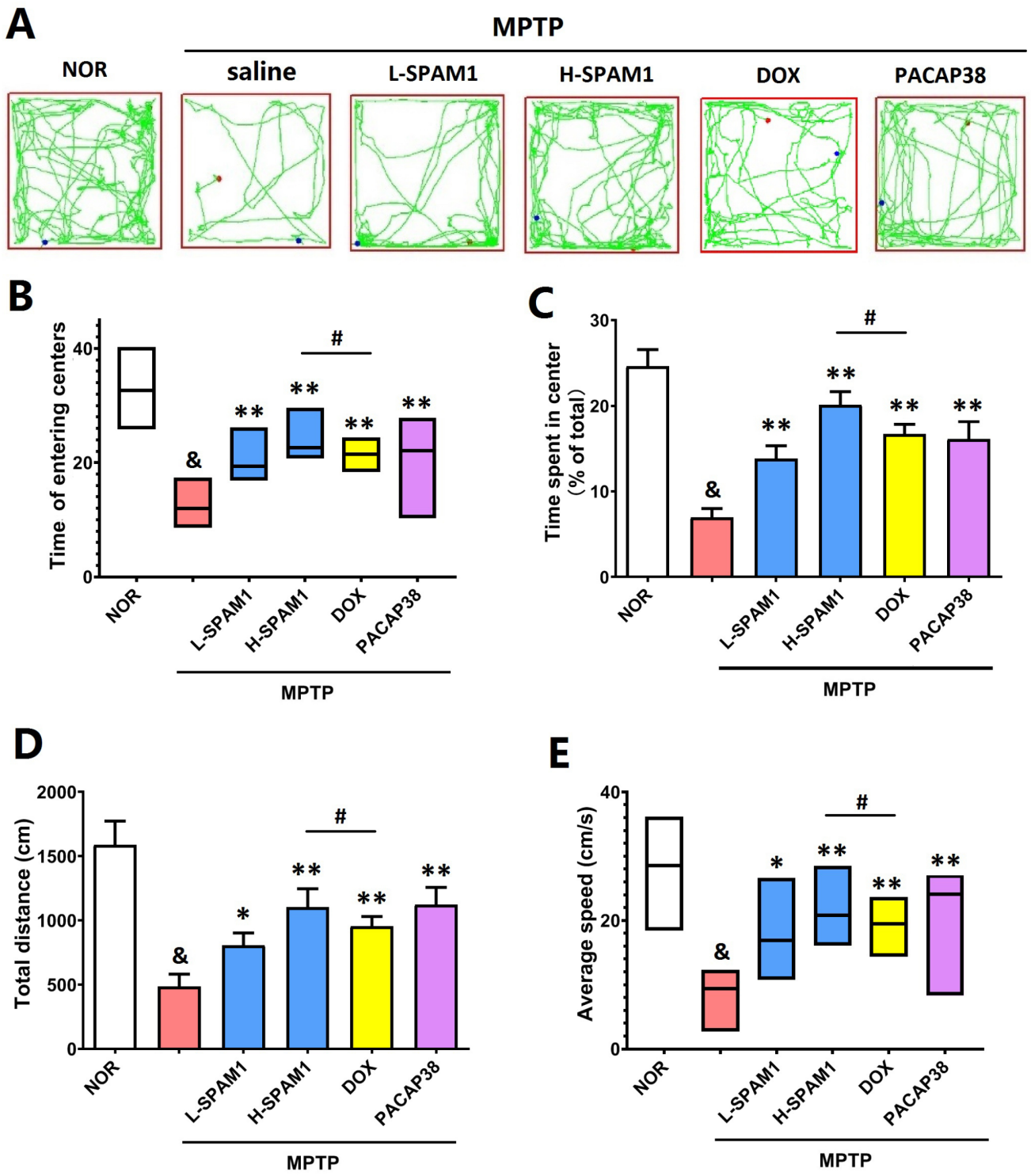

Figure 7. SPAM1 prevents MPTP-induced locomotor and exploratory behavioral deficits The OF test was used to assess the locomotor and exploratory behaviors of mice after 14 days of MPTP treatment. Representative track maps generated from MouBeAt software illustrate the locomotor pattern of mice during 5 min spent in the OF (A). Exploratory behavior was determined by measuring the number of entries into the center (B) and the total time (C) each mouse spent in the center quadrant. Locomotor activity was assessed by comparing the total distance travelled (D) and average speed (E) of mice. $^{\&}P<0.05$, MPTP group vs control group (NOR); $^{*}P<0.05$, vs MPTP group; $^{**}P<0.01$, vs MPTP group; $^{\#}P<0.05$, DOX vs H-SPAM1. Data are presented as the mean ± SEM, $n=10$.

SPAM1 works better than DOX at higher concentrations with fewer side effects.

It has been reported that MPTP significantly decreases the expression of PAC1-R in the basal ganglia of macaque monkeys [22]. Similarly, we also found that the expression of PAC1-R in the substantia nigra and striatum was downregulated by MPTP, which is

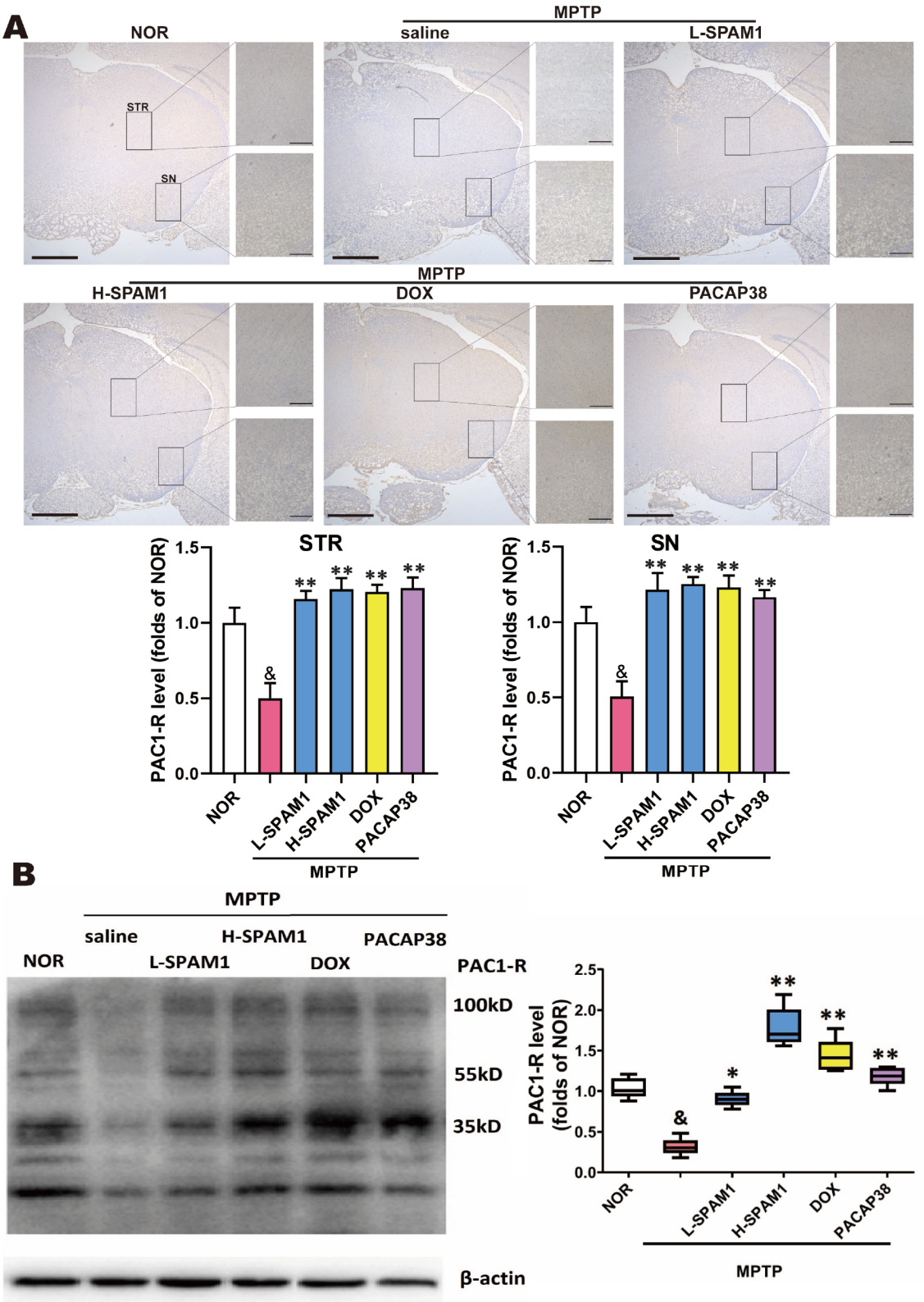

Figure 8. Effects of L-SPAM1, H-SPAM1, DOX, and PACAP38 on the levels of PAC1-R in MPTP-treated mouse substantia nigra and striatum (A) Immunoreactivity and quantitative measurement of PAC1-R staining intensity in the mouse substantia nigra and striatum. SPAM1 and DOX treatment significantly increased the levels of PAC1-R in the substantia nigra and striatum compared with the MPTP group, while SPAM1 worked in a dose-dependent manner. (B) The western bolt images of PAC1-R in striatum and the corresponding statistical analysis showed that L-SPAM1, H-SPAM1 and DOX increased the levels of PAC1-R in striatum compared with the MPTP group. $^{\&}P < 0.05$, MPTP group vs control group (NOR); $^{*}P < 0.05$, vs MPTP group; $^{**}P < 0.01$, vs MPTP group. Data are presented as the mean ± SEM of three experiments. Scale bars: left, 500 μm; right, 100 μm. STR (striatum), and ST (substantia nigra).

consistent with the damaging effects of MPTP on the brain tissues [23,24]. PACAP has been recognized to exert significant neuroprotective activity against most neurotoxic agents [25], in this study we found for the first time that the effect of PACAP38 is associated with the upregulation of PAC1-R. It is known that the upregulation of PAC1-R is an enhancement of neuroprotective activity mediated by PACAP in neurons [26]. Meanwhile, as positive allosteric modulators of PAC1-R, PACAP(28–38) and TAT induce the nuclear translocation of PAC1-R and upregulate PAC1-R expression [27]. Hence, the increase of PAC1-R level induced by PAC1-R's full ligand PACAP38 and its SPAMs, including SPAM1 and DOX, hints that there is a self activity regulation mechanism of PACAP/PAC1-R, which deserves further exploration.

As we know, MPTP treatment severely impairs spine densities [28] and survival of newborn neurons in the dentate gyrus, producing depressive-like behaviors [29]. The defects in exploratory behavior and locomotor behavior in the OF experiment can characterize the depression of the mice. It is well known that PACAP and PAC1-R can protect against the development of depressive behavior [30], while doxycycline also has an anti-depression effect [31]. Here, we noticed that SPAM1, DOX and PACAP38 have significant positive activities against the depression behavior of mice induced by MPTP, while the effect of H-SPAM1 is better than that of DOX and PACAP38. All these results indicate that SPAM1 may be developed as a potential therapeutic agent against not only neurodegenerative diseases but also depression disorders.

In summary, a novel small molecule positive allosteric modulator named SPAM1 was successfully screened out by virtual screening and laboratory experiments in this study. The successful screening of SPAM1 not only confirmed the existence of the positive allosteric modulation site in the N-terminal extracellular domain of PAC1-R, which enhances the neuroprotective activity of PACAP/PAC1-R but also offers a potent drug as an effective neuroprotective agent against neurodegenerative diseases, depression disorders and other nerve damages, which targets PAC1-R with fewer side effects.

Supplementary Data

Supplementary data is available at *Acta Biochimica et Biphysica Sinica* online.

Acknowledgement

We thank the virtual screening and molecular docking service from Prof. Jian Zhang at Shanghai Jiao Tong University School of Medicine (Shanghai, China).

Funding

This work was supported by the grants from the National Natural Science Foundation of China (Nos. 31100545 and 31670848) and the Natural Science Foundation of Guangdong Province (Nos. 2016A030313087 and 2022A1515011158).

Conflict of Interest

The authors declare that they have no conflict of interest.

References

1. Miyata A, Arimura A, Dahl RR, Minamino N, Uehara A, Jiang L, Culler MD, *et al.* Isolation of a novel 38 residue-hypothalamic polypeptide which stimulates adenylate cyclase in pituitary cells. *Biochem Biophys Res Commun* 1989, 164: 567–574
2. Margerin L, Campillo M, Van Tiggelen BA, Hennino R. Energy partition of seismic coda waves in layered media: theory and application to Pinyon Flats Observatory. *Geophys J Int* 2009, 177: 571–585
3. Martínez C, Arranz A, Juarranz Y, Abad C, García-Gómez M, Rosignoli F, Leceta J, *et al.* PAC1 receptor: emerging target for septic shock therapy. *Ann New York Acad Sci* 2006, 1070: 405–410
4. Seaborn T, Masmoudi-Kouli O, Fournier A, Vaudry H, Vaudry D. Protective effects of pituitary adenylate cyclase-activating polypeptide (PACAP) against apoptosis. *Curr Pharmaceutical Des* 2011, 17: 204–214
5. Chang MY, Rhee YH, Yi SH, Lee SJ, Kim RK, Kim H, Park CH, *et al.* Doxycycline enhances survival and self-renewal of human pluripotent stem cells. *Stem Cell Rep* 2014, 3: 353–364
6. Sirenko S, Yang D, Li Y, Lyashkov AE, Lukyanenko YO, Lakatta EG, Vinogradova TM. Ca^{2+}-dependent phosphorylation of Ca^{2+} cycling proteins generates robust rhythmic local Ca^{2+} releases in cardiac pacemaker cells. *Sci Signal* 2013, 6: ra6
7. Bourgault S, Vaudry D, Dejda A, Doan ND, Vaudry H, Fournier A. Pituitary adenylate cyclase-activating polypeptide: focus on structure- activity relationships of a neuroprotective peptide. *Curr Med Chem* 2009, 16: 4462–4480
8. Yang R, Jiang X, Ji R, Meng L, Liu F, Chen X, Xin Y. Therapeutic potential of PACAP for neurodegenerative diseases. *Cell Mol Biol Lett* 2015, 20: 265–278
9. Krakauer T, Buckley M. Doxycycline is anti-inflammatory and inhibits staphylococcal exotoxin-induced cytokines and chemokines. *Antimicrob Agents Chemother* 2003, 47: 3630–3633
10. Kholmukhamedov A, Czerny C, Hu J, Schwartz J, Zhong Z, Lemasters JJ. Minocycline and doxycycline, but not tetracycline, mitigate liver and kidney injury after hemorrhagic shock/resuscitation. *Shock* 2014, 42: 256–263
11. Adembri C, Selmi V, Vitali L, Tani A, Margheri M, Loriga B, Carlucci M, *et al.* Minocycline but not tigecycline is neuroprotective and reduces the neuroinflammatory response induced by the superimposition of sepsis upon traumatic brain injury. *Crit Care Med* 2014, 42: e570–e582
12. Sultan S, Gebara E, Toni N. Doxycycline increases neurogenesis and reduces microglia in the adult hippocampus. *Front Neurosci* 2013, 7: 131
13. Li C, Yuan K, Schluesener H. Impact of minocycline on neurodegenerative diseases in rodents: a meta-analysis. *Rev Neuroscis* 2013, 24: 553
14. Santa-Cecília FV, Leite CA, Del-Bel E, Raisman-Vozari R. The neuroprotective effect of doxycycline on neurodegenerative diseases. *Neurotox Res* 2019, 35: 981–986
15. Yu R, Zheng L, Cui Y, Zhang H, Ye H. Doxycycline exerted neuroprotective activity by enhancing the activation of neuropeptide GPCR PAC1. *Neuropharmacology* 2016, 103: 1–15
16. Song S, Wang L, Li J, Huang X, Yu R. The allosteric modulation effects of doxycycline, minocycline, and their derivatives on the neuropeptide receptor PAC1-R. *Acta Biochim Biophys Sin* 2019, 51: 626–636
17. Baell J, Walters MA. Chemistry: chemical con artists foil drug discovery. *Nature* 2014, 513: 481–483
18. Yu R, Yang Y, Cui Z, Zheng L, Zeng Z, Zhang H. Novel peptide VIP-TAT with higher affinity for PAC1 inhibited scopolamine induced amnesia. *Peptides* 2014, 60: 41–50
19. Zhao W, Zhang R, Ma C, Qiu M, Gong P, Liu Y, Shao S, *et al.* Study on the wound healing, anti-inflammation and anti-bacterial activities of Jinjianling cream: a Chinese herbal compound. *Pakistan Journal of Pharmaceutical Sciences* 2019, 32(3 Special): 1361–1370
20. Gourlet P, Vandermeers A, Vandermeers-Piret MC, De Neef P, Robberecht P. Addition of the (28–38) peptide sequence of PACAP to the VIP sequence modifies peptide selectivity and efficacy. *Int J Peptide Protein Res* 1996, 48: 391–396

21. Poujol de Molliens M, Létourneau M, Devost D, Hébert TE, Fournier A, Chatenet D. New insights about the peculiar role of the 28–38 C-terminal segment and some selected residues in PACAP for signaling and neuroprotection. *Biochem Pharmacol* 2018, 154: 193–202
22. Feher M, Gaszner B, Tamas A, Gil-Martinez AL, Fernandez-Villalba E, Herrero MT, Reglodi D. Alteration of the PAC1 receptor expression in the basal ganglia of MPTP-induced parkinsonian macaque monkeys. *Neurotox Res* 2018, 33: 702–715
23. Bao XJ, Wang GC, Zuo FX, Li XY, Wu J, Chen G, Dou WC, *et al*. Transcriptome profiling of the subventricular zone and dentate gyrus in an animal model of Parkinson's disease. *Int J Mol Med* 2017, 40: 771–783
24. Kuroiwa H, Yokoyama H, Kimoto H, Kato H, Araki T. Biochemical alterations of the striatum in an MPTP-treated mouse model of Parkinson's disease. *Metab Brain Dis* 2010, 25: 177–183
25. Reglodi D, Tamas A, Jungling A, Vaczy A, Rivnyak A, Fulop BD, Szabo E, *et al*. Protective effects of pituitary adenylate cyclase activating polypeptide against neurotoxic agents. *Neurotoxicology* 2018, 66: 185–194
26. Yu R, Lin Z, Ouyang Z, Tao Z, Fan G. Blue light induces the nuclear translocation of neuropeptide receptor PAC1-R associated with the up-regulation of PAC1-R its own in reactive oxygen species associated way. *Biochim Biophys Acta Gen Subj* 2021, 1865: 129884
27. Fan G, Tao Z, Chen S, Zhang H, Yu R. Positive allosteric regulation of PAC1-R up-regulates PAC1-R and its specific ligand PACAP. *Acta Biochim Biophys Sin* 2022, 54: 657–672
28. Weerasinghe-Mudiyanselage PDE, Ang MJ, Wada M, Kim SH, Shin T, Yang M, Moon C. Acute MPTP treatment impairs dendritic spine density in the mouse hippocampus. *Brain Sci* 2021, 11: 833
29. Zhang T, Hong J, Di T, Chen L. MPTP impairs dopamine D1 receptor-mediated survival of newborn neurons in ventral hippocampus to cause depressive-like behaviors in adult mice. *Front Mol Neurosci* 2016, 9: 101
30. Pinhasov A, Nesher E, Gross M, Turgeman G, Kreinin A, Yadid G. The role of the PACAP signaling system in depression. *Curr Pharmaceutical Des* 2011, 17: 990–1001
31. Mello BS, Chaves Filho AJ, Custódio CS, Rodrigues PA, Carletti JV, Vasconcelos SM, Sousa FC, *et al*. Doxycycline at subantimicrobial dose combined with escitalopram reverses depressive-like behavior and neuroinflammatory hippocampal alterations in the lipopolysaccharide model of depression. *J Affective Disord* 2021, 292: 733–745